Holography with conventional LEED

1992 J. Phys.: Condens. Matter 4 999

(http://iopscience.iop.org/0953-8984/4/4/010)

J. Phys.: Condens. Matter 4 (1992) 999–1006. Printed in the UK

Holography with conventional LEED

M A Mendez†, C Glück and K Heinz
Lehrstuhl für Festkörperphysik, University of Erlangen–Nürnberg, Staudtstrasse 7, D-8520 Erlangen, Federal Republic of Germany

Received 8 July 1991, in final form 11 October 1991

Abstract. A recently published interpretation of diffuse LEED patterns as electron holograms as well as the subsequent reconstruction of real-space images is extended to use conventional LEED spot intensities. The procedure is based on the fact that ordered adsorbates produce superstructure spots which sample the diffuse intensity distribution appearing in the case of disordered adsorption. This circumvents experimental difficulties in measuring diffuse (i.e. low-level) intensities, particularly at higher energies. It also opens up the application of electron holography to ordered structures. Using experimental data we show that laterally resolved images can be reconstructed from the spot intensities. However, atomic positions can be displaced and vertical cut images are of insufficient quality.

1. Introduction

Recently a letter by D K Saldin and P de Andres [1] described diffuse intensity distributions emerging from disordered adsorbates in low-energy electron diffraction (LEED) as electron holograms from which atomic real-space images can be reconstructed. The adatom on the surface acts as a microscopic beam splitter which creates the reference wave travelling directly to the detector. The object wave is formed by additional diffraction from the substrate and interferes with the reference wave at the position of the detector. Differences in the path lengths between the two waves are microscopic, so that the limited coherence of the incident electron wave does not matter. The resulting DLEED (diffuse LEED) pattern can be transformed by a phased Fourier transform according to the Helmholtz–Kirchhoff integral [1]. Using this reconstruction procedure a real-space image of the microscopic local adsorption geometry results. The idea originates from a paper by A Szöke [2] and was further developed and tested for photoelectron diffraction patterns by J J Barton [3]. Since then a number of experimental and theoretical papers have appeared and the holographic idea has been extended to Auger electron diffraction and Kikuchi electron patterns, but the proposal of Saldin and de Andres (based on calculated data [1]) is still lacking experimental verification.

Therefore, recently we performed measurements of DLEED patterns for the disordered adsorption of oxygen on Ni(100) at various energies between 400 and 700 eV [4]. One major experimental problem with such measurements comes from the fact that at these higher energies or lower wavelengths (which are recommended to allow for sufficient spatial resolution) the LEED screen is crowded with substrate spots. Their

† On leave from Instituto de Ciencia de Materiales, CSIC, Madrid, Spain.

0953-8984/92/040999 + 08 $04.50

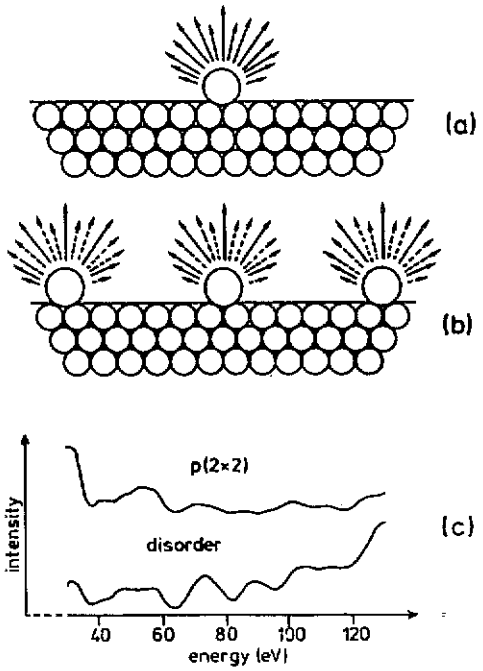

Figure 1. Generation (schematic) of DLEED and LEED intensities (top and middle, respectively) and comparison of their respective energy spectra (bottom).

intensities are orders of magnitude higher than the level of diffuse intensities and, due to their finite spot widths and some blooming of the luminescent screen, they disturb the diffuse intensity distribution considerably. Nevertheless it seems that enough diffuse signal is measurable to allow for a reliable image reconstruction—we report on this in a separate paper [4]. In the present paper, we describe a way to circumvent the experimental difficulties mentioned and we also extend the method of DLEED holography to holography using conventional LEED spot intensities. This opens up the holographic interpretation of adsorbate diffraction to ordered adsorbates as well.

2. Sampling of diffuse intensity distributions

Imagine that there is a single atom or molecule adsorbed on a crystalline substrate. Due to missing translational symmetry the adsorbed scatterer creates a diffuse intensity distribution superimposed on the array of discrete substrate spots. The spatial modulation of this distribution, which is indicated in figure 1(*a*) by different lengths of arrows, carries the information of the local adsorption geometry as demonstrated in a number of recent investigations (for a survey see [5]). If the adsorbate coverage is increased and ordering is allowed the diffuse intensities weaken and contract to form superstructure spots at positions determined by the translational symmetry of the adsorbate. This is schematically shown in figure 1(*b*) where the full line arrows are meant to represent spot directions whilst intensities in directions shown by broken-line arrows cancel by destructive interference. It is clear from this elementary picture that the *relative* intensities emerging in the various directions should not change upon ordering. The idea holds quite generally but of course is only fully true in cases of negligible intra-layer multiple scattering in the adsorbate layer and when the local adsorption geometry is not

affected by ordering. This is approximately true for the system O/Ni(100) which we have investigated recently in its ordered and disordered phases [6]. Though the electron attenuation length is larger than the adatom–adatom distance, neglecting multiple scattering in the adsorbate layer modifies intensities negligibly (checked by test calculations). This is largely due to the normal incidence of the primary beam. So, intensity–energy spectra taken for spot intensities '$I(E)$' and for diffuse intensities '$DI(E)$' taken at equivalent k-space positions should be of similar shape. In fact this is true (as demonstrated in figure 1(c)) for the disordered and the p(2×2) phases of O/Ni(100). Slight differences between the spectra are probably due to increased errors of measurements for the diffuse data. Also, the above arguments for the equivalence of isolated-atom and ordered adlayer intensities hold strictly only for ideal superstructure domains with extensions larger than the electron coherence length. For the case of small disordered domains showing antiphase relations and domain boundaries, the beam intensities may not exactly scale with the single-cluster intensity due to complex interference effects. However, such effects are less important for the integrated spot intensities used here, which are usually less sensitive to disorder than spot profiles. In any case care should be taken to prepare sufficiently large and well ordered superstructure domains. More details concerning the comparison of $I(E)$ and $DI(E)$ spectra can be found in [7].

It is clear from the above finding that, in the absence of intra-adsorbate multiple scattering, superstructure spot intensities provide a sampling grid for diffuse intensities which would emerge for the same local adsorption structure but without long-range order. Consequently, it is sufficient to measure the superstructure spot intensities, provided the grid is dense enough to sample the diffuse intensity distribution completely. The idea of sampling can be found already in Szöke's original paper [2] where an x-ray diffraction pattern is described as a sampled two-dimensional intensity distribution. According to the sampling theorem, the spatial sampling frequency should be twice as large as the modulation frequency observed for the diffuse intensities. For single-atom adsorbates, as in the present case of O/Ni(100), the intensities arise from an area around the adsorbate atom whose diameter is of the order of the electron attenuation length, λ_{in}. The latter is described by the optical potential, V_{oi}, yielding $\lambda_{in} = k/2V_{oi}$ where k is the modulus of the electron wavevector. Typical values are: $V_{oi} = 5$ eV; energies of the order of several hundreds of electronvolts; and λ_{in} of the order of 6 Å (i.e. about twice as much as the unit cell dimension of, for example, Ni(100)). This means that, in agreement with experimental observation, we have about one maximum along a linear axis in the Brillouin zone. We should have two sampling points for this so a p(2×2) array of superstructure spots is just sufficient to sample diffuse intensities safely. We should mention, however, that the spatial variation of diffuse intensities is much faster for large-molecule adsorbates. In this case, the intensities originate from all atoms of the molecule already by kinematic scattering, i.e. they come from a larger area in real space and therefore introduce more structure in reciprocal space. However, ordered superstructures from large molecules create large supercells which in turn cause a denser grid of superstructure spots (again allowing for reliable sampling). A more detailed investigation of how densely diffuse intensities should be sampled is published separately [8].

At this point it is important to stress the fact that only the superstructure spots sample the diffuse intensity distribution. Substrate spots can arise from the substrate only, i.e. they can be dominated by scattering processes which have never encountered the adsorbate species. With respect to holography, this means that the reference wave is not well defined at the positions of the substrate spots. Consequently they must be left out

of the sampling procedure and the intensities at their positions should be replaced by data interpolated from the neighbouring fractional-order spots.

3. Results

We have applied the above idea of sampling diffuse intensities to p(2×2)O/Ni(100). This adsorbate system was experimentally prepared as described earlier [9]. The superstructure spot intensities were taken from a conventional luminescent screen at 80 K using a video camera operated under computer control [10, 11]. The p(2×2) superstructure spot intensities were measured at several electron energies varying between 400 eV and 900 eV whereby the highest order superstructure spot was $\frac{3}{2}0$. No data were taken at the positions of the substrate spots. Instead, values interpolated from the grid of superstructure spot intensities were used as discussed in the previous section. So, a sampling grid of four points per reciprocal substrate unit mesh was provided. As shown explicitly elsewhere [8], this is just enough to sample the intensity distribution reliably. At the highest energy (with the $\frac{3}{2}0$ beam being the highest order spot available) the sampling grid density was given by a 19×19 array of points. To test the appearance of aliasing effects due to insufficient sampling [12], we interpolated the measured grid to a 32×32 array of points using a cubic-spline interpolation scheme. This showed that interpolation was not important for the final result. Figure 2 shows examples of interference patterns for different electron energies.

The sampled intensity distributions were entered into the Helmholtz–Kirchhoff integral, [1, 3] yielding

$$A(\boldsymbol{r}) = \int I(k,\boldsymbol{k}) \exp[-\mathrm{i}kz(1-k_x^2-k_y^2)^{1/2}] \exp[-\mathrm{i}k(xk_x+yk_y)]\,\mathrm{d}k_x\,\mathrm{d}k_y \tag{1}$$

$$= \sum_{i,j} I(k,\boldsymbol{k}_{ij}) \exp[-\mathrm{i}kz(1-k_x^2-k_y^2)^{1/2}] \exp[-\mathrm{i}k(xk_{xi}+yk_{yi})] \tag{2}$$

whereby the unit wave vectors $\boldsymbol{k}_{ij} = (k_{xi}, k_{yj})$ represent the sampling points (i, j). We used a FFT algorithm [12] to calculate summation (2) above. The intensity

$$I(k,\boldsymbol{k}) = |R|^2 + RO^* + R^*O + |O|^2 \tag{3}$$

results from interference between the reference wave, $R \sim F_0(k,\boldsymbol{k})$, and the object wave, $O \sim \Sigma\, F_n(k,\boldsymbol{k})$, whereby indices 0 and n indicate the reference and object (substrate) atoms, respectively. If both the factors, F_0 and F_n, are isotropic and if $|Q|^2$ can be neglected, then the transform $A(\boldsymbol{r})$ is expected to peak at the atomic positions of both the real and the twin image [1–3].

From a detailed LEED structure determination [9] we know that the oxygen atoms reside in hollow positions 0.80 Å above the Ni(100) surface. The adatom is supposed to be the reference atom, so we evaluated (2) for $z = -0.80$ Å to 'see' the nickel atoms in the first layer. Figure 3 displays $|A(\boldsymbol{r})|^2$, as reconstructed from data measured at 426 eV, 710 eV and 820 eV, using a non-linear intensity scale. In the centre of the frames the oxygen signal shows up brightly even 0.80 Å below its true position. This large signal is due to the average intensity of the hologram (as suggested in [2]) and can be reduced by subtraction of the average from the intensity distribution prior to entering the transform. More importantly, however, the nickel atoms surrounding the oxygen adatom show up clearly in the reconstructed images in figure 3. The crosses mark their true location as

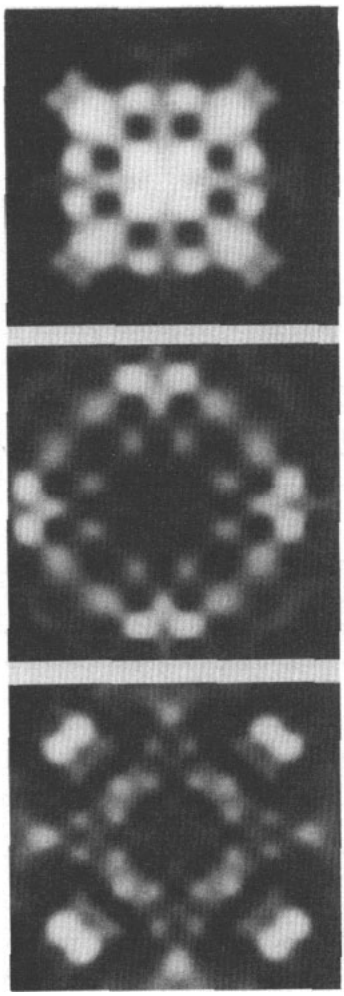

Figure 2. DLEED diffraction patterns at 426 eV, 710 eV and 820 eV (from top to bottom) as constructed from a sampling grid of superstructure spots from p(2 × 2)O/Ni(100).

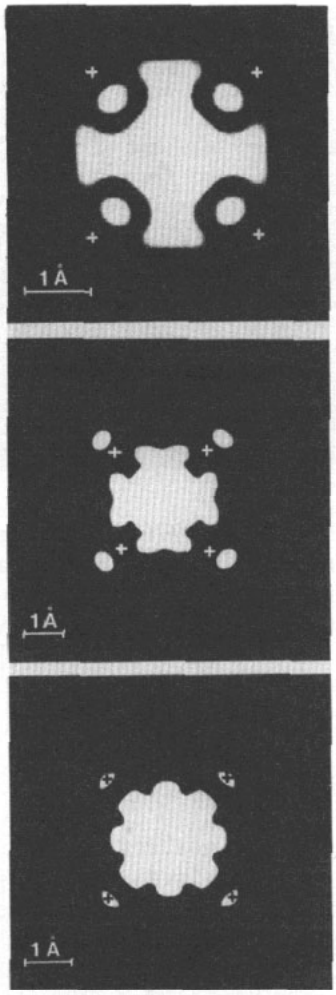

Figure 3. Holographic images for a cut through a plane parallel to the surface and 0.8 Å below the reference oxygen atom (bright centre). The energies used are 426 eV, 710 eV and 820 eV (from top to bottom). Expected atomic positions are marked by crosses.

known from the structural analysis [9]. Evidently, it is only the 920 eV data set for which the true and reconstructed locations coincide. For the other two energies there is a slight shift off the true positions both towards and away from the oxygen atom. Similar shifts were also observed in images reconstructed from calculated diffuse intensities as apparent from figure 3(*a*) of reference [1].

Although the resolution of images parallel to the surface can be of satisfactory quality (as demonstrated in figure 3), the resolution in vertical cut images (i.e. the resolution vertical to the surface) is disappointing. At single energies we get confusing images with

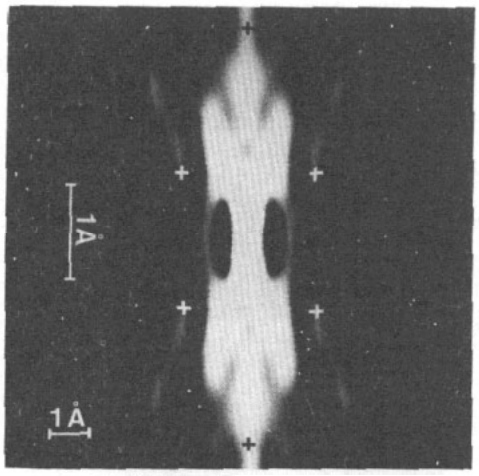

Figure 4. Holographic image taken for a plane perpendicular to the surface passing through an oxygen atom and two of its neighbouring nickel atoms. The underlying data were taken at 820 eV. The upper half of the image is the twin image. Expected positions of nickel atoms are marked by crosses.

elongated bright areas which are only poorly, or not at all, correlated to the expected locations of atoms. Figure 4 gives an example for an electron energy of 820 eV. The twin image is included and the crosses mark the true locations of the first- and second-layer nickel atoms near the adatom. Again the situation is similar to that for images reconstructed from theoretical data [1], which also show bright areas with poor or no correspondence to atomic positions.

4. Discussion

The above experimental results are in full agreement with the features found in the earlier theoretical study of DLEED holography by Saldin and de Andres [1]. This shows the equivalence of both procedures, i.e. the reliable sampling of diffuse intensities by superstructure spot intensities. As for the DLEED case we find for the images reconstructed from LEED data that image cuts parallel to the surface show the four atoms surrounding the oxygen atom with good resolution. However, the positions of the atoms can be displaced from their real positions depending on the electron energy chosen. More disappointing, however, is the quality of vertical cut images which, again in agreement with other holographic work using DLEED-electrons, photoelectrons, Auger or Kikuchi electrons, do not reproduce atomic positions and show a variance of spurious features.

It was suggested in [1] that erroneous features in the images could be reduced by averaging images, $|A(\boldsymbol{r})|^2$, calculated from data at different energies. This is because the true image should not depend on energy, and so true signals should increase but erroneous ones should weaken by the statistics of averaging. Indeed, using theoretical data, averaging was shown to increase the image quality [1]. In agreement with this result is our observation that nickel-atom images can be displaced towards and away from the expected position (figure 3), thus averaging over a larger set of images should work.

However, averaging seems to be only a cosmetic improvement. There must be a serious reason for the displacements and the bad vertical image quality observed. One reason could be that $A(\boldsymbol{r})$ represents the wave amplitude in the sample rather than the

atomic positions. However, it is more likely that the assumptions made in [1] and in the last section for the interpretation of DLEED patterns as holograms do not strictly hold. The main assumptions made are that:

(i) the amplitude of the object wave should be small compared to the amplitude of the reference wave, and

(ii) the variation with $\boldsymbol{K}_{\parallel}$ of both the reference wave and the dynamic-scattering amplitudes of the substrate atoms constituting the object wave should be weak compared to the variation of $\exp(i\boldsymbol{K} \cdot \boldsymbol{r})$.

It has been pointed out recently in a careful investigation by Saldin *et al* [13] that condition (i) is unlikely to hold in the case of forward scattering, i.e. when the object wave is generated by forward scattering of the reference wave originating from an atom deeper in the surface. In this case the term $|O|^2$ in (3) is not negligible and the Fourier transform of the diffraction pattern corresponds to the autocorrelation function rather than to an image of the surface structure. Also, forward-focusing effects dominate the main features of the diffraction intensities. It was emphasized in the same paper [13] that from this point of view the back-scattering case is much more favourable, i.e. the case when the reference wave originates from an atom above the surface and the object wave is generated by the back scattering of the reference wave by the substrate. In fact, as a surface scatters back only a small part of an incident electron wave at the energies under discussion, condition (i) should be satisfied, i.e. the quantity $|Q|^2$ in (3) can be neglected.

We should emphasize that this is true even including all multiple scattering processes within the substrate and between the substrate and the adsorbate. Any electron arriving at the detector has encountered either the adsorbate species or a substrate atom in its last scattering event and so belongs either to the reference or to the object wave. So, the whole problem is shifted to the question of isotropy or anisotropy of the scattering factors, i.e. to the condition (ii). However, the complexity of all multiple scattering processes makes it hard to judge on a quantitative scale to what extent (ii) is satisfied. In the single scattering case there would be some hope of satisfying condition (ii) because the scattering anisotropy is less pronounced in backward scattering than in forward scattering [13]. Also, multiple scattering could decrease the anisotropy further because the different LEED waves coming back from the crystalline substrate impinge on the adsorbate species from many different directions. However, in spite of these positive but very qualitative arguments, condition (ii) must be violated in the present case because of the observed image quality described above.

This raises the question of suitable corrections in the image-reconstruction formulae (1, 2) to account for the obvious anisotropy of factors F_0 and F_n. Promising proposals were published recently which correct the measured intensities either by kinematic scattering factors [13–15] or, in the forward-scattering case, by avoiding data generated in direct forward-focusing processes [16]. It was shown, particularly for the backward scattering case which applies in this work, that the kinematic scattering-factor correction works surprisingly well. However, application to real data is still lacking though our group plans to consider this in the future.

Finally, it is fair to point out that DLEED or LEED holography can become valuable structural tools only when the necessary refinements in the image-reconstruction procedure are less complex than traditional full dynamic $I(E)$ or DLEED calculations. Otherwise, there is no advantage in the holography technique. However, in view of the progress made recently [13–16] we feel that there is some hope that the refinements need only be crude compared to the demands of full dynamic-scattering calculations. In this

case, (D)LEED holography would provide a fast and reliable initial idea about a surface structure, whose details could be detected by subsequent refinement through conventional methods, e.g. by conventional LEED structure determination.

Acknowledgments

We appreciate financial support by Deutsche Forschungsgemeinschaft (DFG) and the European Science Foundation (ESF). MAM is indebted to the Spanish Government for an FPI grant and for financial support through CICYT. We would also like to thank Dr Pedro de Andres (CSIC, Madrid) and Professor D K Saldin (University of Wisconsin, Milwaukee) for stimulating and helpful discussions.

References

[1] Saldin D K and de Andres P L 1990 *Phys. Rev. Lett.* **64** 1270
[2] Szöke A 1986 Short wavelength coherent radiation: generation and applications *AIP Conf. Proc.* vol 147, ed D J Atwood and J Boker (New York: American Institute of Physics)
[3] Barton J J 1988 *Phys. Rev. Lett.* **61** 1356
[4] Mendez M A, Guerrero J, Glück C, de Andres P L, Heinz K, Saldin D K and Pendry J B 1991 *Phys. Rev.* B submitted
[5] Heinz K 1990 *Vacuum* **41** 328
[6] Oed W, Starke U, Heinz K, Müller K and Pendry J B 1991 *Surf. Sci.* **251/252** 488
[7] Heinz K, Starke U and Bothe B 1991 *Surf. Sci.* **243** L70
[8] Heinz K, Starke U, Van Hove M A and Somorjai G A 1991 *Surf. Sci.* at press
[9] Oed W, Lindner H, Heinz K, Müller K, Saldin D K, de Andres P L and Pendry J B 1990 *Surf. Sci.* **225** 242
[10] Heinz K and Müller K 1982 *Structural Studies of Surfaces* (*Springer Tracts in Modern Physics 91*) ed G Höhler (Berlin: Springer)
[11] Heinz K 1989 *Prog. Surf. Sci.* **27** 239
[12] Press W H, Flannery B P, Tenkolsky S A and Vetterling W T 1986 *Numerical Recipes* (Cambridge: Cambridge University Press)
[13] Saldin D K, Harp G R, Chen B L and Tonner B P 1991 *Phys. Rev.* B **44** 2480
[14] Tong S Y, Wei C M, Zhao T C, Huang H and Li H 1991 *Phys. Rev. Lett.* **66** 60
[15] Tonner B P, Han Z-L, Harp G R and Saldin D K 1991 *Phys. Rev.* B **43** 14423
[16] Thevuthasan S, Herman G S, Kaduwela A P, Saiki R S, Kim Y J, Niemczura W, Burger M and Fadley C S 1991 *Phys. Rev. Lett.* **67** 469